Creep, Stress Rupture, and Isothermal Aging of Reinforced Polyphthalamide

JED S. LYONS,* EDGARDO G. TINIO, and SCOTT F. BERRY

Department of Mechanical Engineering, University of South Carolina, Columbia, South Carolina 29208

SYNOPSIS

The effects of time, temperature, and particulate filler on the tensile behavior of short fiber-reinforced polyphthalamide (PPA) were investigated experimentally. Creep and stress-rupture characteristics and tensile properties before and after isothermal aging were determined. Temperatures ranged from 23 to 150°C and tests lasted up to about 4000 h. Stress-rupture master curves were created, using a WLF-type analysis, which can be used for interpolation with reasonable accuracy. Creep rates were low but were affected by increased moisture absorption in the lowest temperature environment. All properties were affected by chemical degradation of the PPA matrix at the highest temperature. Under most conditions investigated, the mineral filler improved the creep resistance and stiffness of the PPA resin at the expense of strength and ductility. Scanning electron microscopy examinations of fractured specimens indicated that the mineral filler embrittled the matrix and may have damaged the fibers during processing. © 1995 John Wiley & Sons, Inc.

INTRODUCTION

Polyphthalamide (PPA) is a semicrystalline thermoplastic created from aliphatic diamines and terephthalic acid.[1] PPA resins have excellent mechanical and physical properties and chemical resistance at ambient and elevated temperatures.[2,3] The incorporation of short fibers, mineral particulate fillers, and impact modifiers aims to further improve upon the properties of the PPA matrix without causing processing difficulty. Developed to provide improved performance without higher cost, PPA resins are suitable for automotive applications, such as the water outlet of a passenger car engine.[4]

Since under-the-hood temperatures can exceed 100°C for periods of several hours, it is critical to be able to predict the effects of stress, temperature, and time on the deformation behavior of the material. However, a systematic study of these relationships for glass fiber- and mineral particulate-reinforced PPA injection-molding resins has not been reported in the literature. The primary objective of this project was to provide the needed design information. The approach taken combined experimental tensile, creep, and stress-rupture property determinations with scanning electron microscopy examinations. The reported results can assist in the development of PPA-based materials with improved high-temperature mechanical characteristics.

EXPERIMENTAL

Materials

Two commercially produced polyphthalamide thermoplastic resin systems, designated PPA-G and PPA-GM, were injection-molded into ASTM D638-82A[5] Type I, $\frac{1}{16}$ in.-thick tension specimens. The resin designated PPA-G was reinforced with 45% chopped E-glass fiber; PPA-GM contained 40% glass and also 25% mineral (calcium–silicate) particulate. The fiber length, diameter, and surface treatment were the same for the two materials. The matrix material of both resins was a heat-stabilized semicrystalline polyphthalamide containing a 3.2 wt % reactive thermoplastic elastomer as a modifier. The glass transition temperature, T_g, of the matrix was about 95°C at 50% relative humidity.[6]

One of two heat-treatment schedules was applied to the dry-as-molded specimens: annealing or annealing followed by isothermal aging. First, every

* To whom correspondence should be addressed.

Journal of Applied Polymer Science, Vol. 56, 1169–1177 (1995)
 CCC 0021-8995/95/091169-09

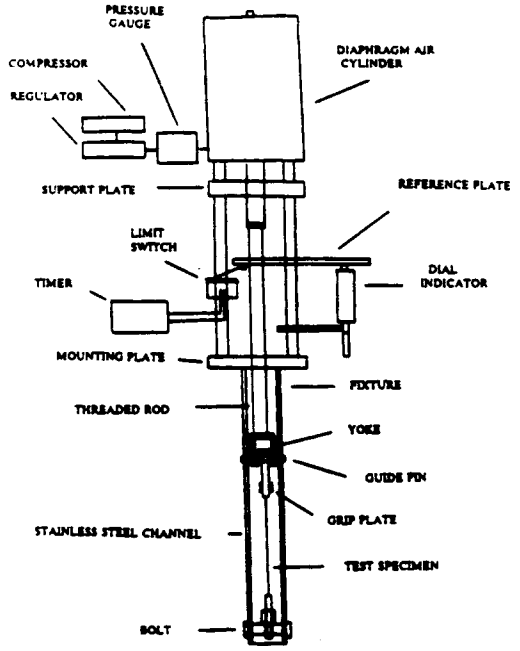

Figure 1 Schematic illustration of loading fixture used for stress rupture and creep testing.

specimen was annealed in air for 2 h at 160°C, then air-quenched to room temperature prior to testing. This reduced residual stresses from the molding process and the effects of aging during storage. This relatively high annealing temperature was selected because the materials were semicrystalline and heavily reinforced, which broadens the temperature range of the glass transition.[7] Second, a group of annealed specimens were isothermally aged at 65, 100, and 150°C for 50, 200, 500, 2000, or 5000 h. Two samples per material were aged at each condition. The effects of aging time and temperature were subsequently evaluated by tensile testing.

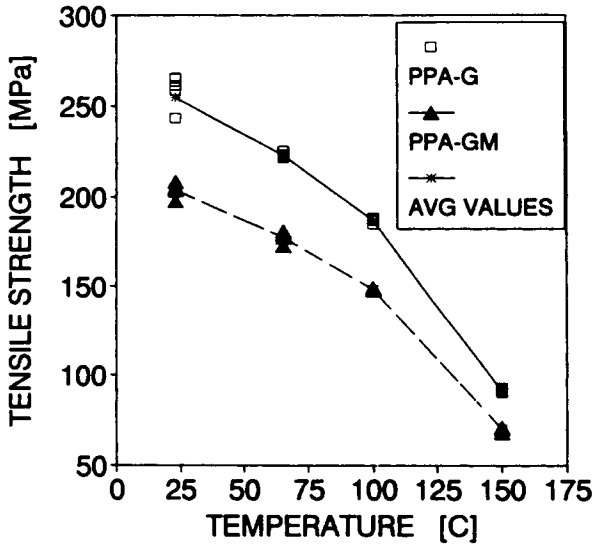

Figure 2 Effect of temperature on the tensile strength of annealed PPA-G and PPA-GM.

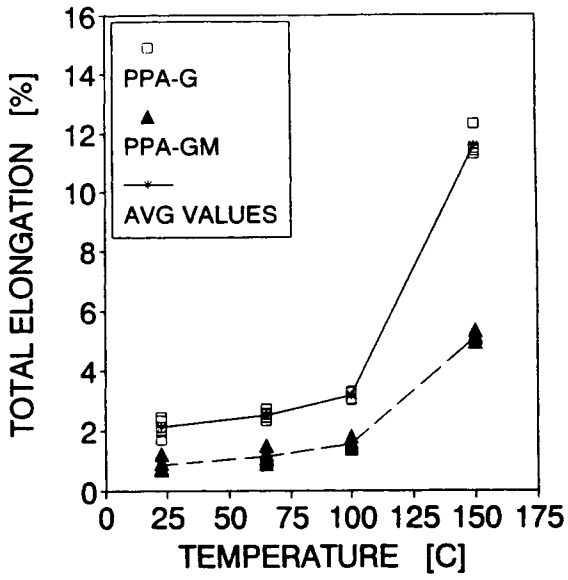

Figure 3 Effect of temperature on the total elongation of annealed PPA-G and PPA-GM.

Tensile Testing

Tension tests were performed using a 22 kN capacity Tinius Olsen universal testing machine and 23–450°C LabTemp oven. Wedge-loading grips were used, and the test speed was 0.2 in./min. Five as-annealed samples were tested at temperatures of 23, 65, 100, and 150°C. Tension testing of the specimens which were isothermally aged was conducted at the respective aging temperatures. This was done in order to compare the effects of aging alone to the combined effects of aging and creep that occur during stress-rupture testing.

Each sample was held at a temperature for a minimum of 1 h prior to testing. Material properties were extracted from the load-displacement curves. The secant elastic modulus was measured at a stress of 20.7 MPa. The tensile strength was calculated from the maximum load and the original specimen dimensions. Ductility was quantified by the total elongation at fracture.

Stress-rupture Testing

Constant load stress-rupture tests were performed at 23, 65, 100, and 150°C using equipment developed at the University of South Carolina[8,9] and shown schematically in Figure 1. These loading frames were

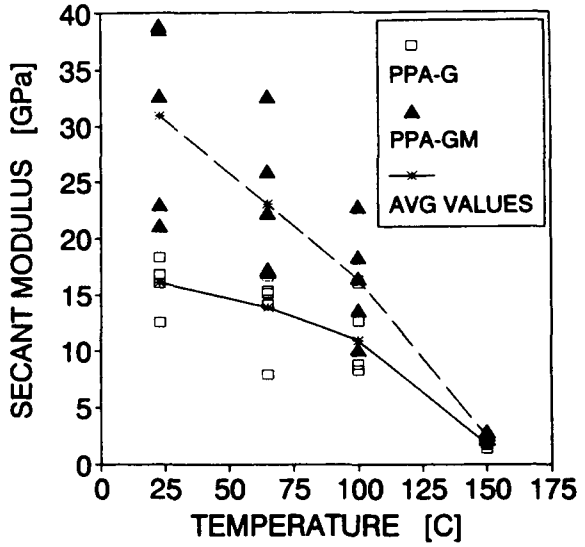

Figure 4 Effect of temperature on the secant modulus of annealed PPA-G and PPA-GM.

pneumatically actuated and allowed the specimen and grips to extend into a forced-air convection oven. When a specimen in a loading station broke, the reference plate was pulled upward, releasing the limit switch and stopping the timer clock. The time-to-rupture, t_R, of the specimen was then recorded from the timer clock, and the station was reset to conduct another test with a different specimen at a different stress level.

Test temperatures were maintained to ±3°C or better. Prior to starting the tests, all loading stations were calibrated using a 0–440 kN load cell. The load applied by the air cylinder was controlled to better than ±0.8 kN. Thus, the worst-case uncertainty in the applied stress was about ±5% at 21 MPa.

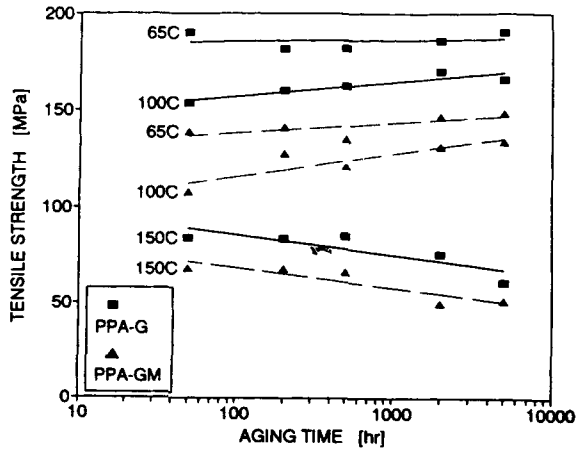

Figure 5 Effect of aging on the ultimate tensile strength of PPA-G and PPA-GM.

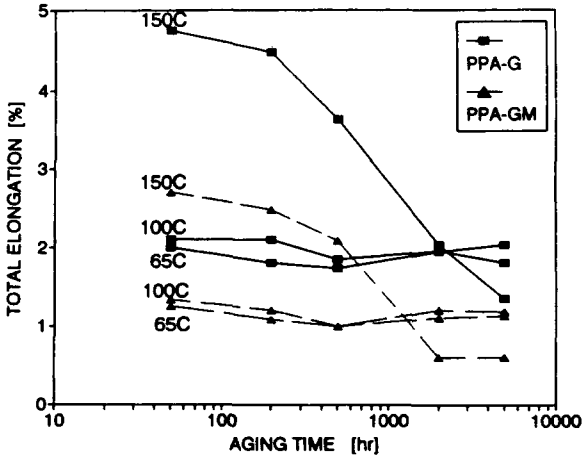

Figure 6 Effect of aging on the total elongation of PPA-G and PPA-GM.

Creep Testing

Constant load creep tests of ~ 4000 h duration were performed using applied stress levels of 20.7 and 41.4 MPa. One sample per material was tested at each stress level at three temperatures: 23, 100, and 150°C. Elevated temperature creep tests were conducted using pneumatically actuated loading frames similar to those used for stress-rupture testing, except the timers were replaced by dial gauges with 0.0254 mm resolution. Dead-weight, lever-arm-type loading frames with identical dial gauges were used to measure creep deformation at 23°C in an environmental chamber under 50% relative humidity conditions.

Microscopic Examinations

A Hitachi 2500Δ scanning electron microscope (SEM) was used to characterize the fracture surfaces

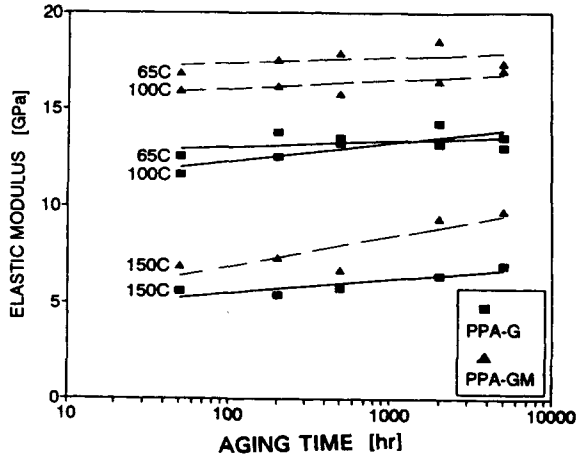

Figure 7 Effect of aging on the secant elastic modulus of PPA-G and PPA-GM.

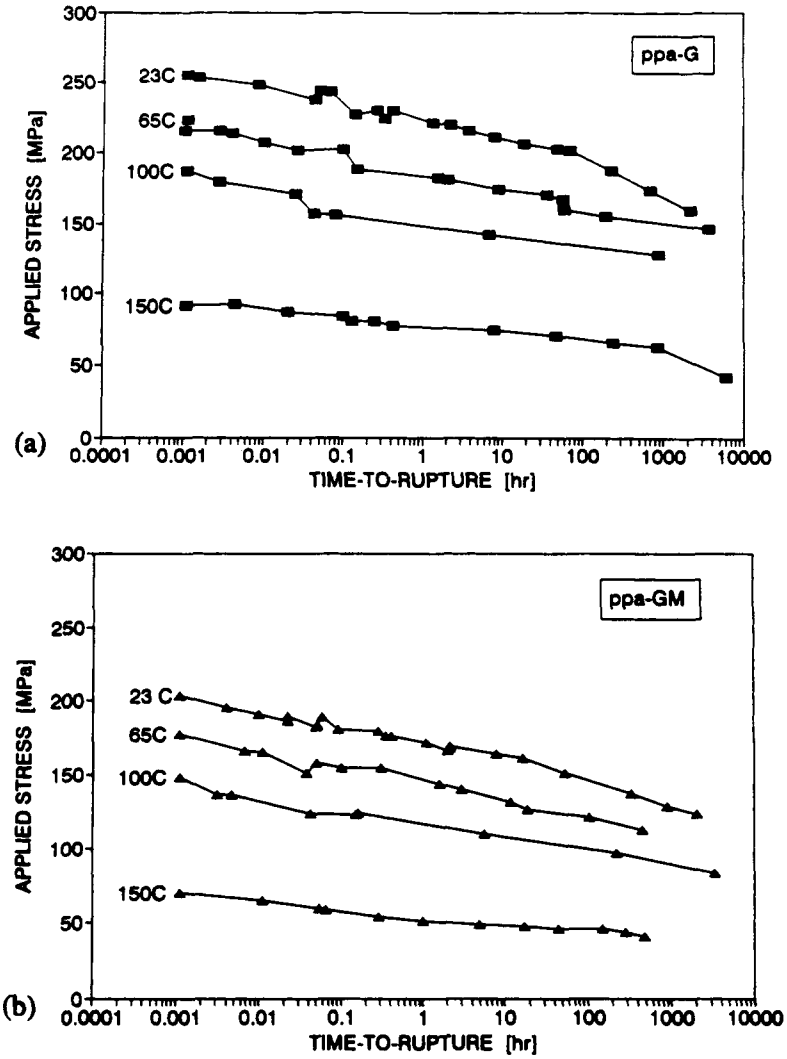

Figure 8 Effects of stress and temperature on time-to-rupture for (a) PPA-G and (b) PPA-GM.

of tested samples. Fiber pullout lengths, l_P, were estimated from direct measurements on the SEM CRT screen of at least 50 fibers on each sample. Also, an Olympus PME3 reflected light microscope and a LECO 1001 image analyzer were used to measure the fracture surface profile roughness, R_L. The surface profile roughness was calculated from the true fracture surface profile length divided by the projected length.[10] Larger R_L values signify greater fracture surface areas and generally correspond to tougher materials.

RESULTS

Tensile Properties

All tensile test specimens fractured catastrophically at the ultimate load during testing, with no measurable change in cross-section dimensions. Tensile properties measured within 24 h after annealing are presented in Figures 2–4. Room-temperature tensile strengths were 2–2.5 times greater than that of neat PPA, confirming the value of fiber and particulate reinforcement. As can be seen in Figures 2 and 3, PPA-G was consistently stronger and more ductile than was PPA-GM. Although PPA-GM has slightly less fiber than does PPA-G, the difference in ultimate strength is more likely due to the presence of the mineral filler in PPA-GM. Such particulates act as stress concentrators during loading.

The effect of temperature on the ultimate properties of the two materials was similar. Increased temperature resulted in a continual reduction in strength. Figure 3 shows that the total elongation to fracture was nearly temperature-independent up to 100°C, above which it increased significantly. A

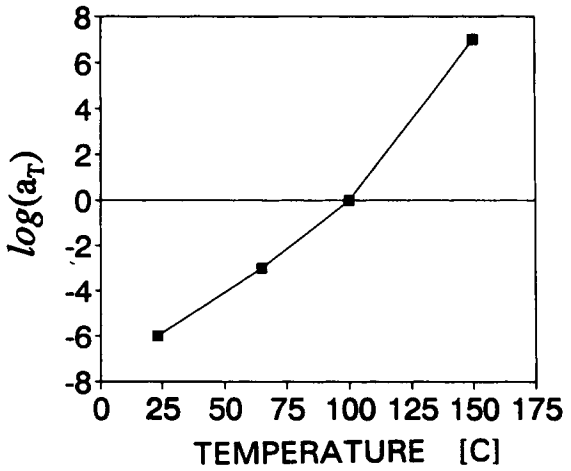

Figure 9 Temperature-dependent shift factors used for stress-rupture master curves.

significant amount of scatter is present in the secant modulus results, as can be seen in Figure 4. This scatter is attributed to uncertainties in small strain measurements. However, by comparing average values, it is clear that between 23 and 100°C PPA-GM is stiffer than is PPA-G. Increased temperature decreased the secant modulus of both materials. The stiffness of PPA-GM decreased with increased temperature more rapidly than that of PPA-G. If fact, at 150°C, which is above T_g, secant modulus values for the two materials were nearly equal.

Tensile properties after isothermal aging are plotted vs. aging time in Figures 5–7. Aging affected the properties of PPA-G and PPA-GM in similar ways: Aging at 65 or 100°C caused the tensile strengths and the secant moduli to increase slightly with aging time. Aging at 100°C caused more rapid property changes than did aging at 65°C. These observations indicate that a gradual continuation of the glass transition occurred in the PPA matrix after the annealing heat treatment.

Aging at 150°C resulted in a general deterioration of mechanical properties. Although the stiffness was increased, significant decreases in the strength and ductility of the each material with aging time were observed. This result is likely due to thermal oxidation of the PPA matrix, which was observable as discoloration of the specimens.

Stress-Rupture Properties

Applied stresses were varied to give rupture lifetimes ranging between 0.001 and 4000 h. Graphs of applied stress vs. time-to-rupture are presented in Figure 8. For both the glass-reinforced and glass-plus-mineral-reinforced PPA resins, increases in either the applied stress or the test temperature resulted in decreased times-to-rupture. However, Figure 8 clearly shows that for a given stress level and temperature PPA-G had a longer lifetime than that of PPA-GM. These results suggest that the mineral filler weakened the material. Because the mineral particulates are elastic heterogeneities in the PPA matrix, they can concentrate stress and, hence, act as sites for void nucleation.

To facilitate the interpretation of the results, master curves were created from the stress and time-to-rupture data using the WLF time–temperature equivalence theory.[11,12] The reference temperature was 100°C, which is close to the matrix T_g at 50% RH of the PPA matrix. Simple horizontal shifts on the time scale were applied to the

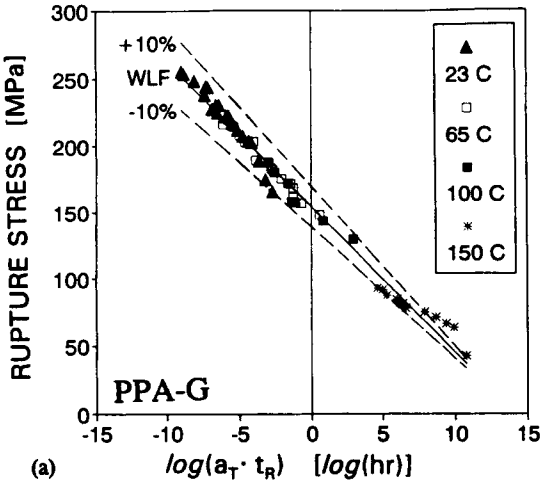

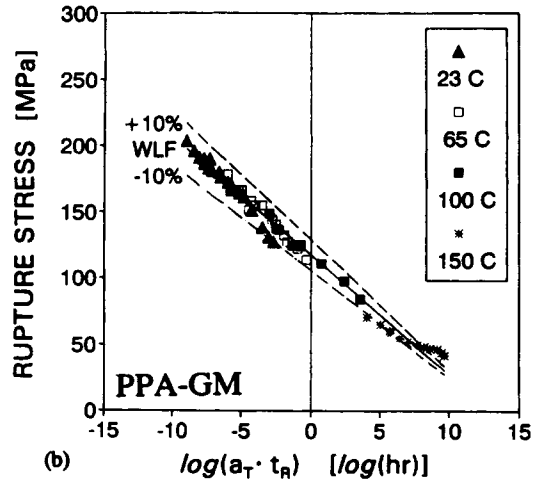

Figure 10 WLF master curves for stress-rupture of (a) PPA-G and (b) PPA-GM.

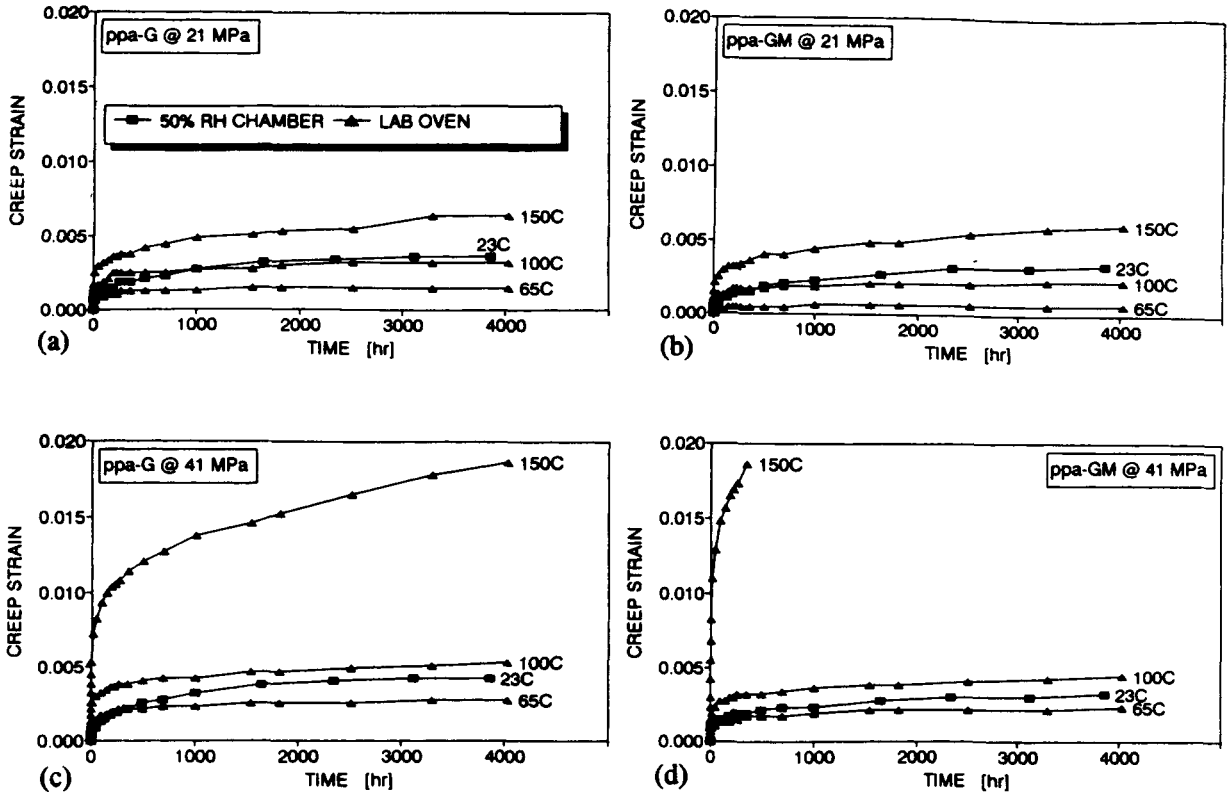

Figure 11 Creep strains due to a 21 MPa applied stress for (a) PPA-G and (b) PPA-GM and a 41 MPa applied stress for (c) PPA-GM and (d) PPA-GM.

stress–time rupture data. The shift factor, a_T, was determined empirically to depend on temperature, as shown in Figure 9. The resulting stress-rupture master curves are presented in Figure 10. In each of these graphs, the best-fit straight line through the data is labeled "WLF." Two dashed lines indicating ±10% error from the best fit line are also included.

It is clear that a nearly linear relationship exists between the rupture stress of PPA-G or PPA-GM and the reduced time variable $\log(a_T \times t_R)$. It seems that the fiber and particulate reinforcements broadened the effective glass transition temperature range of the resins, so that a radical change in material behavior did not occur over the temperature range investigated. However, close inspection of Figure 9 or 10 reveals that the slope of the stress-rupture data obtained at 150°C is slightly less than the average slope. This is attributed to increased creep of the polymer matrix and to the chemical degradation processes that were observed during isothermal aging at 150°C. Thus, the master curves presented here should not be used for extrapolating stress-rupture properties. However, they can be used with reasonable accuracy for interpolation at temperatures between 23 and 150°C.

Creep Properties

In general, both PPA-G and PPA-GM were resistant to creep. Results of the creep tests are shown in Figure 11, where creep strain is plotted vs. time. Under most testing conditions, the material response consisted of (a) a primary creep stage of about 500–1000 h duration during which time the creep strain rate decreased, followed by (b) a steady-state stage where the creep rate remained nominally constant during the remainder of the test. In the temperature range of 23–100°C, the resin containing the mineral filler was more resistant to creep than was the resin which contained only glass. However, the opposite was true at 150°C. In fact, the PPA-GM sample tested at an applied stress of 41 MPa and temperature of 150°C exhibited only a transient creep stage and ruptured in less than 500 h. This result is consistent with the stress-rupture results, indicating that the mineral filler was detrimental to the load-bearing capacity of the PPA when the temperature is well above the polymer's T_g.

To quantify the effects of stress and temperature on the creep behavior of the materials, the steady-state creep strain rate was calculated from the linear portions of the creep curves. Always, the creep rate

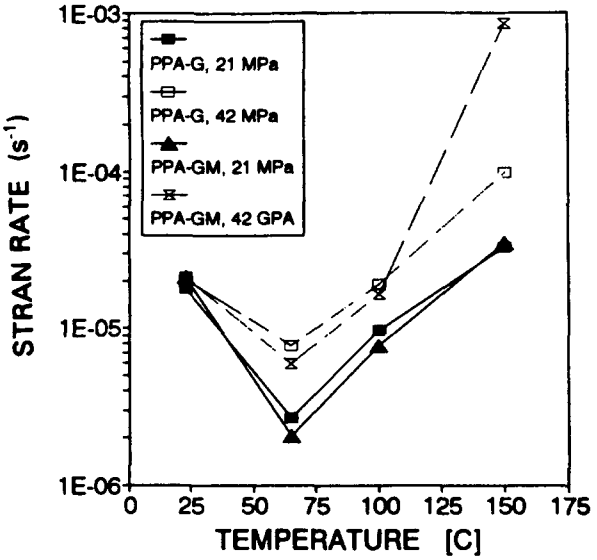

Figure 12 Steady-state strain rates of PPA-G and PPA-GM during creep testing.

was observed to increase as the applied stress was increased. However, as shown in Figure 12, the test temperature seemed to have an unusual effect on the steady-state creep rate of both materials. Between 65 and 150°C, the creep rate increased with temperature, as expected. However, the measured creep rate at 23°C was greater than that measured at 65°C. All specimens were tested in the dry-as-annealed condition, but tests at 23°C were done in a 50% RH environmental chamber. Thus, these samples may have absorbed moisture to reach equilibrium with the environment. The makeup air for the ovens used for elevated temperature tests was drawn from a room at ambient conditions, so the relative humidity in the oven chambers was less than 50%. Further, the deformations measured at 23°C are apparently independent of stress level and material type. This evidence suggests that the dimensional changes measured at room temperature were caused primarily by swelling due to moisture absorption and that the true creep rate at 23°C is smaller than could be measured.

An additional concern is that the creep specimens tested at 65 and 100°C probably aged while they crept. The continued glass-transition mechanism that occurred during aging may have caused the material to become more resistant to creep as the test proceeded. At 150°C, chemical degradation of the matrix may also have affected the creep rate. These phenomena precluded the application of WLF-type analyses or classical viscoelasticity to describe the experimental data. The investigators are currently conducting additional research in this area.

DISCUSSION

In general, PPA-GM was stiffer but weaker and more brittle than was PPA-G. The fracture surfaces of tension and stress-rupture test specimens were characterized using the SEM in order to determine the roles of temperature and time on the failure process. For either material after either test at any temperature, the failure mode was a mixture of fiber fracture (in-plane with the matrix crack) and fiber pullout. Small holes were observed in the matrix, which is indicative of impact modifier debonding.[13] Thus, the basic failure mechanisms were not affected by the parameters varied in this research. However, the extent to which each mechanism contributed to the global constitutive behavior was affected by the presence of the particulate filler and by the test temperature.

Table I contains quantitative fractography results. Despite the large amount of scatter in the measurements, trends in the data are clear. The R_L values indicate that the fracture surface of PPA-G was slightly rougher than that of PPA-GM. Increased temperature resulted in increased roughness. SEM examinations revealed that increases in fracture surface roughness were due to (a) increased ductility of the PPA matrix and (b) increased fiber

Table I Fracture Surface Characterization Parameters

	Pullout Length Avg ± STD (μm)		Profile Roughness Avg ± STD	
Test Type	PPA-G	PPA-GM	PPA-G	PPA-GM
Tension, 23°C	63 ± 22	43 ± 17	1.9 ± 0.4	1.7 ± 0.3
Tension, 150°C	83 ± 40	52 ± 16	2.3 ± 0.5	1.9 ± 0.2
Stress rupture, 23°C	56 ± 23	31 ± 14	1.7 ± 0.3	1.7 ± 0.3
Stress rupture, 150°C	80 ± 25	46 ± 9	2.3 ± 0.3	1.8 ± 0.7

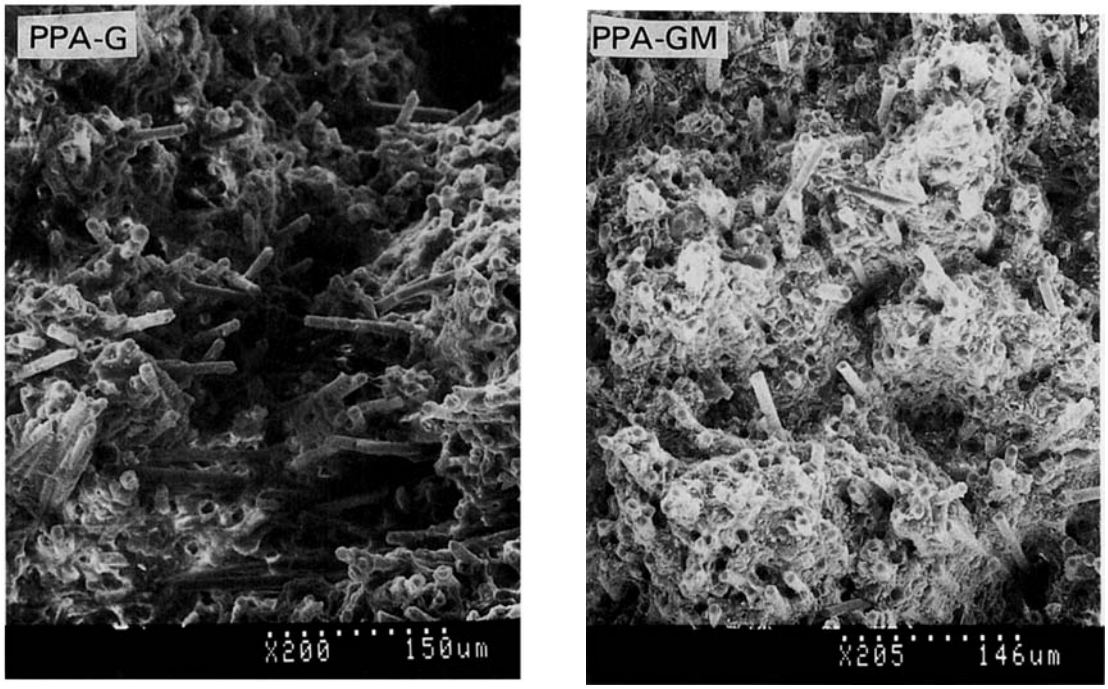

Figure 13 Fracture surfaces of PPA-G and PPA-GM after tensile testing at 150°C.

pullout lengths. In PPA-GM, the mineral filler particles promoted flat fracture in the matrix by nucleating small, closely spaced voids which linked up to cause material failure. As the temperature was increased, the roughness increased slightly due to the matrix becoming more rubbery and tough. The test duration did not affect the roughness parameter significantly.

Fiber pullout lengths were shorter for PPA-GM than for PPA-G, as exemplified by the SEM photomicrographs in Figure 13. It is known that the pullout length is primarily controlled by fiber size and strength and by the interface bond strength. However, the fibers in the two materials were originally the same length, diameter, and composition and obtained the same surface treatment prior to incorporation into the resin. This suggests that the mineral filler in PPA-GM decreased the amount of fiber pullout length. The particles may have damaged the fibers during processing and/or molding, lowering their strength and promoting fiber failure close to the matrix crack.

It was observed that there were more protruding fibers aligned parallel to the stress axis in the long-term stress-rupture specimens than in the short-term tension tests. This is evidence of creep deformation of the polymer prior to rupture. The measured data also indicate that increased temperature resulted in increased pullout lengths, as can be seen by comparing the fracture surfaces from tension tests of PPA-G at 23 and 150°C in Figure 14. As the matrix softened, the fibers could pullout to a greater length before being stressed to their ultimate strength. The material with the greater pullout length (PPA-G) also had the higher ductility and tensile strength, indicating greater utilization of the fiber reinforcement.

CONCLUSION

New, quantitative information was determined regarding the time- and temperature-dependent tensile behavior of two polyphthalamide resin systems containing impact modifier, glass fibers, and mineral particulates. As the test temperature was increased, the strength and stiffness of the materials decreased while the ductility and creep rate increased. Anomalous time-dependent strain accumulation occurred during creep testing at 23°C, probably due to moisture absorption. At 150°C, chemical degradation of the PPA matrix affected all the measured properties. In the temperature range from 23 to 100°C, the mineral-filled glass fiber-reinforced material was weaker but stiffer and more creep resistant than was the material which did not contain the mineral filler. At 150°C, the mineral filler had detrimental effects on all mechanical properties and caused premature failure. The particulates acted as sites for void nucleation during loading and apparently reduced the fiber aspect ratio during compounding.

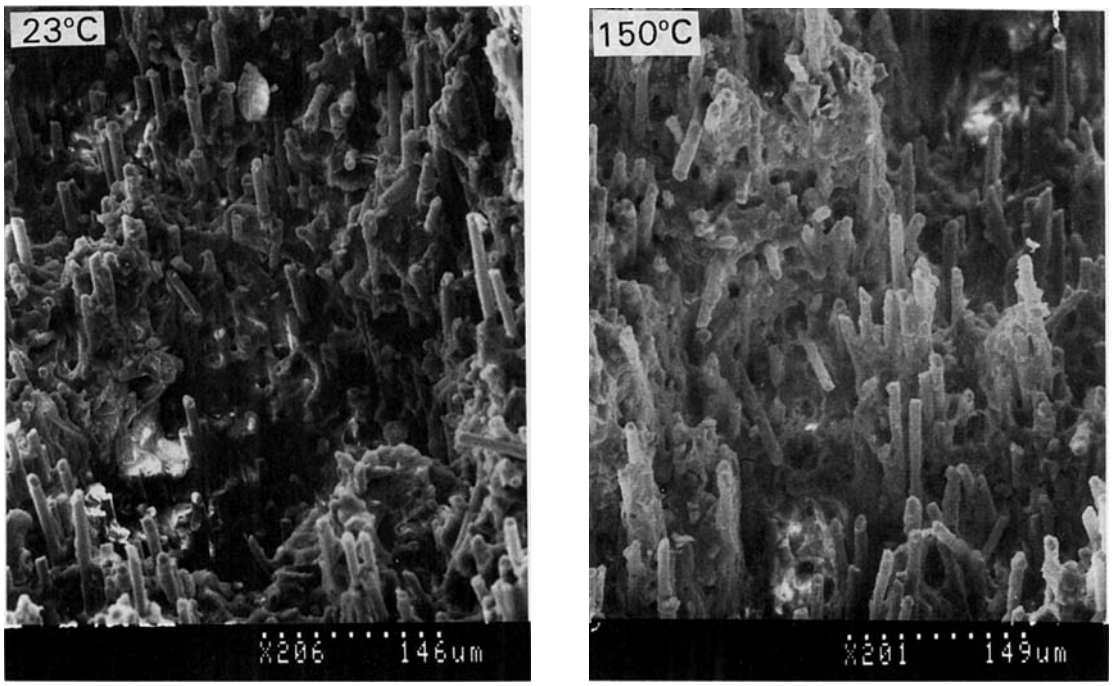

Figure 14 Fracture surfaces of PPA-G after ~ 750 h stress-rupture tests at 23 and 150°C.

Amoco Performance Products, Inc., is thanked for providing financial support for E. T. and S. B. and for supplying the materials for this research.

REFERENCES

1. D. Erickson, *Sci. Am.*, **265**(5), 130 (1991).
2. M. H. Naitove, *Plast. Technol.*, **37**(4), 45 (1991).
3. A. S. Wood, *Modern Plastics*, **68**(2), 24 (1991).
4. S. Ashley, *Mech. Eng.*, **116**, 29 (1994).
5. ASTM Designation D 638-82a Standard Test Method for Tensile Properties of Plastics, *Annual Book of ASTM Standards*, 1984.
6. Amoco Performance Products Inc., *AMODEL® PPA Resins Engineering Data and Design Manual*, APPI, Alpharetta, GA, 1994.
7. L. C. E. Struik, *Physical Aging in Amorphous Polymers and Other Materials*, Elsevier, Amsterdam, 1978.
8. G. K. Ajit, Master's Thesis, University of South Carolina, 1990.
9. T. Deng, Master's Thesis, University of South Carolina, 1991.
10. E. E. Underwood, *Fracture Mechanics: Microstructure and Micromechanisms*, ASM International®, Metals Park, OH, 1989, p. 87.
11. M. L. Williams, R. F. Landel, and J. D. Ferry, *J. Am. Chem. Soc.*, **78**, 3701 (1955).
12. T. L. Smith, *J. Polym. Sci.*, **32**, 99 (1958).
13. L. J. Moskala, *J. Mater. Sci.*, **27**, 1883 (1992).

Received September 20, 1994
Accepted December 13, 1994